D. Mackenzie

C. Nadarajah

J. Shi

J. T. Boyle

Department of Mechanical Engineering,
University of Strathclyde,
Glasgow, Scotland, U.K.

Simple Bounds on Limit Loads by Elastic Finite Element Analysis

A method for bounding limit loads by an iterative elastic continuum finite element analysis procedure, referred to as the elastic compensation method, is proposed. A number of sample problems are considered, based on both exact solutions and finite element analysis, and it is concluded that the method may be used to obtain limit-load bounds for pressure vessel design by analysis applications with useful accuracy.

1 Introduction

In current practice, pressure vessel design by analysis is most commonly based on elastic finite element analysis and the rules defined in Codes such as the ASME Boiler and Pressure Vessel Code Sections III and VIII (Division 2) [1] and BS5500 [2]. This approach gives rise to two significant problems in the design: elastic analysis is used to assess possible inelastic failure mechanisms and the design by analysis rules are essentially based on shell theory. These problems introduce the concept of *stress categories* into the design procedure: the designer performs the analysis and partitions the calculated stresses into *peak*, *primary* and *secondary* stress categories, each of which is associated with distinct failure mechanisms, (fatigue, gross distortion and ratcheting, respectively) and subject to different limiting values. Code guidelines are given for categorization of stresses at particular locations arising from specific loading; however, these guidelines are often based on shell theory concepts such as membrane and bending stresses which are not directly applicable to 2-D and 3-D solid finite element results. A number of categorization techniques (such as stress linearization [3] and reduced modulus categorization methods [4]) have been proposed to aid the designer in appropriate categorization of stress; however, to date, no satisfactory solution has been found [5, 6] and stress categorization remains problematic.

The foregoing problems essentially arise from current practice: the Code rules in fact allow the designer to circumvent categorization problems by performing *plastic* or *limit* analyses of the component which, unlike elastic analysis, take account of stress redistribution upon yield. (Indeed, it has recently been argued that plastic analysis should be the preferred method for assessing failure modes associated with gross distortion due to a single application of pressure [7].) Plastic and limit analysis can be performed using nonlinear finite element programs; however, nonlinear finite element analysis is intrinsically more difficult to perform than elastic analysis: material models must be defined, the iterative solution procedure must be suitably controlled, and much greater computing resources are required. In order to make the transition from elastic to inelastic or limit-load-based design for real structures, simplified analysis methods are required.

One simplified method for calculating lower-bound limit loads by iterative elastic finite element analysis has previously been presented (see references [8–11]). The *elastic compensation method* was developed from the reduced modulus stress categorization method [12], in which the effects of material inelasticity are simulated by repeated elastic analyses in which the elasticity modulus of the component is systematically reduced at regions of high stress. Marriott proposed that this method could be extended to limit analysis by using modulus reduction techniques in conjunction with the *lower-bound limit-load theorem* [13]. An alternative method of calculating limit loads by repeated elastic analysis has been proposed by Seshadri et al. [14]. In the GLOSS r-node method, statically determinate stresses at locations referred to as r-nodes are identified by iterative elastic analysis in which regions of high stress have their modulus reduced, while regions of low stress have theirs increased. The stresses at the r-node locations are insensitive to the assumed material model and considered to be reference stresses similar to creep reference stresses [15].

The object of the elastic compensation method as defined in references [8–11] is to establish a stress field suitable for substitution into the lower-bound theorem by systematically modifying the local elastic modulus in a finite element model so as to cause the stress to redistribute. Initially a conventional elastic finite element analysis is performed for an arbitrary load set, P_1. This initial homogeneous isotropic solution is taken as iteration zero in a series of linear elastic analyses, in which the elastic modulus of each element is modified according to an expression of the form

$$E_i = E_{(i-1)} \frac{\sigma_n}{(\sigma_{(i-1)})}$$

where subscript i is the iteration number, σ_n a nominal stress value, and $\sigma_{(i-1)}$ the maximum (unaveraged) nodal equivalent stress associated with the element calculated in the previous iteration. This iterative procedure redistributes the stress in the component and over a number of iterations the net effect is

Contributed by the Pressure Vessels and Piping Division for publication in the JOURNAL OF PRESSURE VESSEL TECHNOLOGY. Manuscript received by the PVP Division, June 29, 1992; revised manuscript received November 18, 1992. Associate Technical Editor: M. Moktarian.

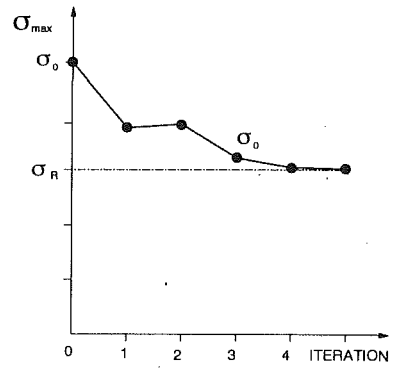

Fig. 1 Maximum stress for each iteration

to decrease the maximum stress in the model as illustrated in Fig. 1.

A lower-bound limit load can then be calculated by invoking the lower-bound limit-load theorem, which states that if a statically admissable stress field in which the stress nowhere exceeds yield exists for a given component under given loading, the loading is a lower bound on the limit load. The elastic compensation solution meets the first requirement of the lower-bound theorem in that it is statically admissible (subject to the usual finite element approximations). As the iteration solutions are linear elastic, the stress magnitude is proportional to the applied load. A lower-bound limit load can therefore be established by calculating the load required to give a maximum (unaveraged) nodal stress equal to the nominal yield strength σ_Y from proportionality. Considering the iteration giving the lowest value of maximum nodal stress σ_R

$$P_L = P_1 \frac{\sigma_Y}{\sigma_R}$$

where P_L is the best estimate of limit load given by the foregoing procedure. The applied load set P_1 is not restricted to single loads and may represent multiple forces, moments, pressures, etc., in the manner of proportional loading in conventional limit analysis. This paper extends the foregoing method to allow calculation of limit-load bounds by considering the upper-bound limit-load theorem.

2 Upper-Bound Limit Loads

The upper-bound limit-load theorem states that if, for a given load set, the rate of dissipation of internal energy in a body is equal to the rate at which external forces do work in any postulated mechanism of deformation, the applied load set will be equal to or greater than the plastic collapse load [16]. Mathematically, a complete plastic collapse solution requires definition of P and σ, an equilibrium set of loads and stresses respectively, and $\dot{\epsilon}$ and $\dot{u}$, a geometrically compatible set of displacement and strain increments, respectively. An upper-bound solution requires only a *partial* or *incomplete* plastic collapse solution to be defined; specifically, $\dot{u}^*$ and ϵ^*, representing any compatible sets of displacement and strain increments, respectively, which define a geometrically possible mode of deformation. The asterisk notation therefore denotes a solution which is incomplete in the sense that the stress field is not defined. Applying virtual work to the problem, it can be shown [16]

$$\Sigma P\dot{u}^* \le \int_V \dot{D}^* dV \tag{1}$$

where $\dot{D}^*$ is the increment of dissipation of energy per unit volume calculated for the incomplete solution. The increment of energy dissipation per unit volume for a Tresca perfectly plastic material is given by the expression

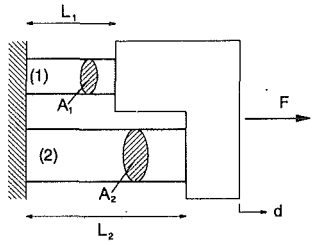

Fig. 2 Two-bar structure

$$\dot{D}^* = \sigma_Y |\dot{\epsilon}^*|_{\max}$$

where $|\dot{\epsilon}^*|$ is the greatest principal strain rate magnitude. In the case of a Mises perfectly plastic material, the more complex expression

$$\dot{D}^* = \sigma_Y \sqrt{\frac{2}{3}(\dot{\epsilon}_1^{*2} + \dot{\epsilon}_2^{*2} + \dot{\epsilon}_3^{*2})}$$

is valid, where $|\dot{\epsilon}_i^*|: i = 1, 2, 3$ are the principal strain rates.

The upper-bound theorem requires the definition of a geometrically possible mode of deformation for the component: essentially, compatible sets of displacement and strain increments must be defined. This is done automatically when the elastic compensation iteration procedure is applied to a finite element model. The elastic compensation procedure results in an anisotropic inhomogeneous linear elastic solution, the compatible displacement and strain fields of which can be used to define a geometrically possible mode of deformation of the structure.

An upper-bound limit load for a structure can be obtained by substituting the elastic compensation displacement increment field $\dot{u}^*$ and strain increment field $\dot{\epsilon}^*$ into the upper-bound theorem as expressed in Eq. (1). However, this approach can lead to practical problems as calculating the work term can be laborious if corresponding load and displacement vectors are not directly accessible in the finite element program, (pressure loads on nonplanar surfaces present particular problems). In practice, it is more convenient to take advantage of the linear elastic nature of the elastic compensation solution: as the solution is elastic, the *external work done* must equal the *elastic strain energy* of the structure; thus

$$\Sigma P\dot{u}^* = \int_V \sigma\dot{\epsilon}^* dV$$

where σ is the elastically calculated stress, and $\dot{\epsilon}^*$ the elastically calculated strain increment. Thus, the upper-bound theorem inequality may be written

$$\int_V \sigma\dot{\epsilon}^* dV \le \int_V \dot{D}^* dV \tag{2}$$

Example 1: Two-Bar Structure. The limit load of a simple two-bar structure as illustrated in Fig. 2 was considered in reference [8], where it was shown that the limit load given by the elastic compensation method was identical to the exact limit load, given by the expression

$$\frac{F_L}{F_Y} = \frac{L_2(A_1 + A_2)}{A_1L_2 + A_2L_1}$$

where F_L and F_Y represent limit load and yield load, respectively. The same result is found if the elastic compensation solution is substituted into the upper-bound limit-load theorem as given in the foregoing. The elastic stress in each bar may be evaluated simply as

$$\sigma_1 = \frac{FE_1L_2}{A_1E_1L_2 + A_2E_2L_1} \qquad \sigma_2 = \frac{FE_2L_1}{A_1E_1L_2 + A_2E_2L_1}$$

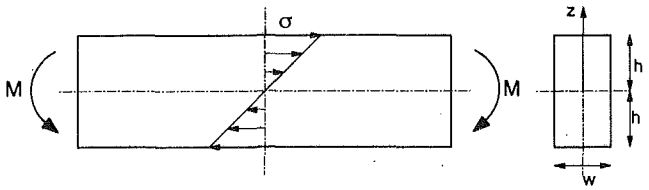

Fig. 3 Beam under pure bending

where initially $E_1 = E_2 = E_o$. Assuming bar 2 to be longer than bar 1, first yield will occur in bar 1 when $F = F_Y$

$$\sigma_1 = \frac{F_Y L_2}{A_1 L_2 + A_2 L_1} = \sigma_Y$$

Using *elastic compensation*, the elastic modulii in the bars are corrected based on the results of the initial elastic analysis according to the expression

$$E_m = E_o \frac{S}{\sigma}$$

where E_m is the modified modulus, E_o is the original modulus, σ the elastically calculated stress in the bar, and S an arbitrarily chosen value of stress. Substituting the expression for corrected modulus into the bar stress equations gives

$$\sigma_1 = \frac{F}{A_1 + A_2} \quad \sigma_2 = \frac{F}{A_1 + A_2}$$

that is, $\sigma_1 = \sigma_2$. Applying the upper-bound theorem to the elastic compensation analysis gives

$$\int_V \sigma \epsilon dV = \int_V \sigma_Y \epsilon dV$$

which simplifies to

$$\sum_{i=1}^{2} \sigma_1 \epsilon_y V_i = \sum_{i=1}^{2} \sigma_Y \epsilon_i V_i \Leftrightarrow \sigma_1 = \sigma_2 = \sigma_Y$$

for the simple bar structure. Substituting the expressions for σ_1, σ_2 and σ_Y into the foregoing gives

$$\frac{F_L}{F_Y} = \frac{L_2(A_1 + A_2)}{A_1 L_2 + A_2 L_1}$$

which agrees with the exact solution.

Example 2: Beam Under Pure Bending. The limit load of a rectangular beam under a pure bending moment as illustrated in Fig. 3 was considered in reference [8], where it was shown that the limit load given by the elastic compensation method was identical to the exact limit load

$$M_L = \frac{3}{2} M_Y$$

The same result is found if the elastic compensation solution is substituted into the upper-bound limit-load theorem as given in the foregoing. Applying the elastic compensation procedure to the beam results in the following strain and stress distributions [8]:

$$\epsilon_{(z)} = \kappa Z = \frac{2}{3} \frac{M^2 z}{E_o \alpha M_Y I}$$

$$\sigma_{(z)} = E_{(z)} \epsilon_{(z)} = \frac{2}{3} \frac{Mh}{I}$$

where E_o is the initial elastic modulus, M_Y the moment at first yield, and α an arbitrary constant such that $0 < \alpha < 1$. Considering symmetry, applying the upper-bound theorem gives

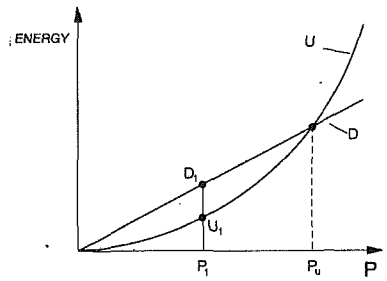

Fig. 4 Plot of strain energy and energy dissipation against applied external load

$$2 \int_0^h \sigma \epsilon dz = 2\sigma_Y \int_0^h \epsilon dz$$

or

$$\frac{4}{9} \frac{M^3 h^3}{E_o \alpha M_Y I^2} = \frac{2}{3} \sigma_Y \frac{M^2 h^2}{E_o \alpha M_Y I}$$

which simplified and rearranged yields the exact limit load

$$M_L = \frac{3}{2} M_Y$$

3 Upper-Bound Limit Loads by FEA

In a linear elastic analysis, the upper-bound theorem may be expressed by inequality (2)

$$\int_V \sigma \dot{\epsilon}^* d\nu \leq \int_V \dot{D}^* dV$$

or

$$U \leq D$$

The strain energy U of a linear elastic body varies with the applied load set squared. The dissipation of internal energy D varies directly with the applied load set. Thus,

$$U = \int_V \sigma \dot{\epsilon}^* d\nu = AP^2 \tag{3a}$$

$$D = \int_V \dot{D}^* dV = BP \tag{3b}$$

Plotting strain energy and energy dissipation against applied external load gives curves of the form shown in Fig. 4.

When the strain energy and energy dissipation curves intersect, the load is an upper bound on the limit load. The intersection can be calculated by performing an analysis for an arbitrary load set P_1 and evaluating the corresponding strain energy U_1 and energy dissipation D_1. Substituting the calculated values into Eqs. (3*a*) and (3*b*) gives

$$A = \frac{U_1}{P_1^2} \quad B = \frac{D_1}{P_1}$$

and the strain energy and energy dissipation may be expressed as

$$U = \frac{U_1}{P_1^2} P^2 \quad D = \frac{D_1}{P_1} P$$

The applied load set P is an upper-bound limit P_u load when $U = D$; that is,

$$\frac{U_1}{P_1^2} P_u^2 = \frac{D_1}{P_1} P_u$$

and, hence, the upper-bound limit load is given by the expression

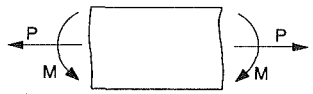

Fig. 5 Beam under combined loading

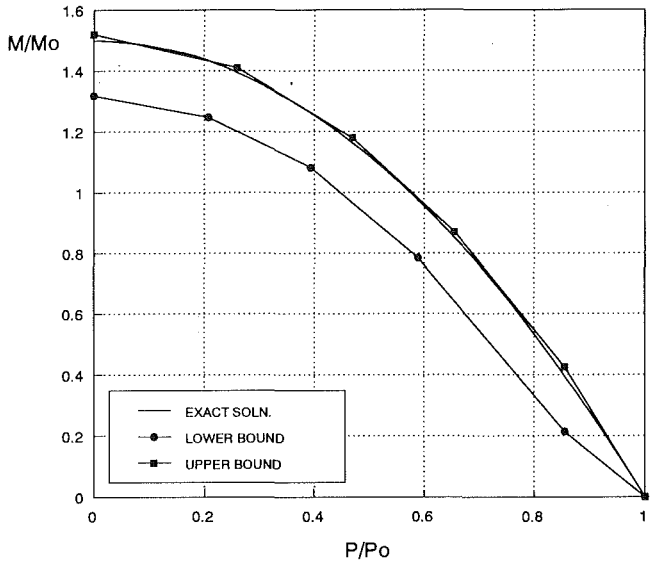

Fig. 6 Beam under combined loading limit-load bounds by iterative elastic analysis

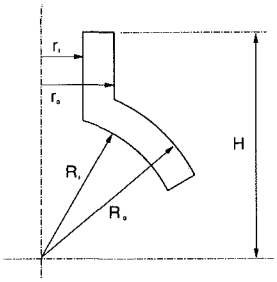

Fig. 7 Nozzle/sphere intersection

$$P_u = \frac{D_1}{U_1} P_1$$

4 FEA Examples

In this section a number of example problems are investigated by finite element analysis using the program ANSYS [17]. The upper-bound solutions calculated in the finite element analysis are **approximate** as the strain energy and energy dissipation integrals are calculated approximately by a summation based on element centroidal data and volume. Nonlinear elastic-plastic finite element analysis, used for comparison purposes, is based on an elastic-perfectly plastic material model.

Beam Under Bending and Tension. As an example of the foregoing, consider a beam of unit width and depth under combined direct and bending loading, as illustrated in Fig. 5. The theoretical collapse load of a cantilever beam of unit width under direct force P and moment M is given by the expression

$$\frac{M}{M_Y} = \frac{3}{2}\left[1 - \left(\frac{P}{P_Y}\right)^2\right]$$

where, for a beam of depth d, $P_Y = \sigma_Y d$ and $M_Y = \sigma_Y d^2/6$.

In the finite element model, 12 linear quadrilateral plane stress elements were taken through the depth of the beam. Up to 8 iterations were performed for each model and the modulus correction equation used throughout was

$$E_i = E_{(i-1)} \frac{20E3}{\sigma_{(i-1)\max}}$$

where $\sigma_{(i-1)\max}$ is the maximum (unaveraged) nodal stress calculated in the previous analysis. The bounded limit surface given by the elastic compensation procedure is compared with the exact solution in Fig. 6.

Table 1 Series A nozzle dimensions

NOZZLE	r_i (mm)	r_o (mm)	R_i (mm)	R_o (mm)	H (mm)
A1	150	155	500	505	600
A2	100	120	500	520	600
A3	250	255	500	520	460
A4	250	260	500	510	550

Table 2 Series A limit pressures (N/mm²)

NOZZLE	Lower Bound	E-P	Upper Bound	Robinson & Gill [9]
A1	2.09	2.34	2.6	2.15
A2	15.9	17.8	18.4	18
A3	5.87	---	6.4	6.48
A4	4.08	---	4.86	4.4

Table 3 Series B nozzle dimensions

NOZZLE	r_i (mm)	r_o (mm)	R_i (mm)	R_o (mm)	H (mm)
B1	150	155	500	505	600
B2	100	120	500	520	600

Table 4 Series B limit pressures (N/mm²)

Specimen	Lower Bound	E-P	Upper Bound	Lower Bound [19]	Upper Bound [19]
B1	47.5	57.5	63.7	33.71	37.46
B2	104.2	117	142.5	170	233.3

Nozzle/Sphere Intersection. Limit-load bounds were calculated for six thin nozzle/sphere intersections. The models were created from higher order (quadratic) axisymmetric elements with three or four elements through wall thickness. The modulus correction equation used was

$$E_i = E_{(i-1)} \frac{200}{\sigma_{(i-1)\max}}$$

where $\sigma_{(i-1)\max}$ is the maximum (unaveraged) nodal stress calculated in the previous analysis.

Series A intersections, defined in Table 1 and Fig. 7, were subjected to internal pressure loading only. Lower and upper-bound limit loads obtained by the elastic compensation procedure are compared with elastic-perfectly plastic finite element analysis, and the lower-bound results of Robinson and Gill [18] in Table 2. Series B intersections, defined in Table 3 and Fig. 7 were subject to radial downward load on the nozzle only.

Lower and upper-bound limit loads obtained by the elastic compensation procedure are compared with elastic-perfectly plastic finite element analysis and with rigid-perfectly plastic analysis upper and lower-bound solutions in which the nozzle was considered to be a rigid boss [19] in Table 4.

Torispherical Head. Limit-load bounds were calculated for four torispherical heads as defined in Fig. 8 and Table 5.

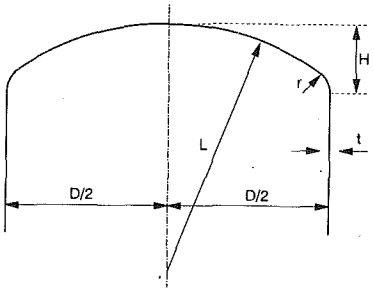

Fig. 8 Torispherical head geometry

Finite element models were created in ANSYS using a uniform mesh with six higher order (quadratic) quadrilateral axisymmetric elements through wall thickness. The modulus correction equation used was

$$E_i = E_{(i-1)} \frac{209}{\sigma_{(i-1)\max}}$$

where $\sigma_{(i-1)\max}$ is the maximum (unaveraged) nodal stress calculated in the previous analysis. The calculated limit-load bounds are compared with the elastic-plastic calculated limit loads (pressure at 1 percent equivalent strain) in Table 6.

5 Discussion and Conclusion

In general, the elastic compensation limit loads calculated in the foregoing sample analyses are found to be of useful accuracy, particularly in the case of the upper-bound loads, which are very close to the inelastically calculated limit load. However, it should be noted that the calculated upper-bound limit loads may not be true upper bounds as the energy integrals calculated in the sample analyses are **approximate** values, based on centroidal stresses and strains. Elements which integrate the energy terms by Gaussian quadrature are currently being developed by a colleague of the writers and it may be that the true upper-bound loads are higher.

The proposed method has several features convenient to the design engineer: it can be implemented automatically in standard linear elastic commerical finite element programs (thus, minimal manual intervention is required) and, unlike nonlinear methods, detailed inelastic material models, loading histories and nonlinear iteration/convergence controls are not required. However, investigation of the procedure is at an early stage and further work is required to examine the effects of mesh density, etc., on the accuracy of the solution [20].

Acknowledgments

This research was funded by the UK Science and Engineering Research Council. Mr. C. Nadarajah is funded by ICI plc. Use of the ANSYS software through an educational license from Swanson Analysis is also acknowledged.

Table 5 Head shape parameters and dimensions

HEAD	t/D	h/D	r/D	R/D	D (mm)	t (mm)
HD31	0.015	0.151	0.092	1.541	940	14
HD32	0.015	0.207	0.070	0.813	940	14
HD4	0.050	0.250	0.125	0.750	940	47
HD26	0.050	0.207	0.125	1.021	940	47

Table 6 Torispherical end limit pressures (N/mm^2)

Head	Lower Bound	Elastic-Plastic	Upper Bound
HD31	2.32	2.88	2.96
HD32	3.71	4.72	5.02
HD26	16.12	19.93	20.75
HD4	21.66	23.61	24.33

References

1 American Society of Mechanical Engineers, ASME Boiler and Pressure Vessel Code, 1989.

2 British Standards Institution, "BS5500: Specification for Unfired Fusion Welded Pressure Vessels," 1991.

3 Kroenke, W. C., "Classification of Finite Element Stresses According to ASME Section III Stress Categories," *Proceedings, 94th ASME Winter Annual Meeting*, 1973.

4 Dhalla, A. K., "A Simplified Procedure to Classify Stresses for Elevated Temperature Service," *Proceedings*, ASME-PVP, Vol. 120, San Diego, Calif., 1987, pp. 177–188.

5 Hechmer, J. L., and Hollinger, G. L., "Three-Dimensional Stress Criteria," ASME PVP, Vol. 210-2, San Diego, 1991, pp. 181–191.

6 Mackenzie, D., and Boyle, J. T., "On Stress Categorization by Reduced Modulus Analysis," ASME JOURNAL OF PRESSURE VESSEL TECHNOLOGY, submitted for publication.

7 Kalnins, A., and Updike, D. P., "Role of Plastic Limit and Elastic-Plastic Analyses in Design," ASME PVP, Vol. 210-2, San Diego, 1991, pp. 135–142.

8 Mackenzie, D., and Boyle, J. T., "A Method of Estimating Limit Loads by Iterative Elastic Analysis. I—Simple Examples," *International Journal of Pressure Vessels and Piping*, Vol. 53, No. 1, 1993, pp. 77–95.

9 Nadarajah, C., Mackenzie, D., and Boyle, J. T., "A Method of Estimating Limit Loads by Iterative Elastic Analysis. II—Nozzle Sphere Intersections With Internal Pressure and Radial Load," *International Journal of Pressure Vessels and Piping*, Vol. 53, No. 1, 1993, pp. 97–119.

10 Shi, J., Mackenzie, D., and Boyle, J. T., "A Method of Estimating Limit Loads by Iterative Elastic Analysis. II—Torispherical Heads Under Internal Pressure," *International Journal of Pressure Vessels and Piping*, Vol. 53, No. 1, 1993, pp. 121–142.

11 Mackenzie, D., Shi, J., Nadarajah, C., and Boyle, J. T., "An Iterative Elastic Analysis Procedure for Estimating Lower-Bound Limit Loads," *Proceedings*, ASME PVP, New Orleans, La., 1992.

12 Jones, G. L., and Dhalla, A. K., "Classification of Clamp Induced Stresses in Thin-Walled Pipe," *Proceedings*, ASME PVP-Vol. 81, New York, N.Y., 1981.

13 Marriott, D. L., "Evaluation of Deformation or Load Control of Stresses Under Inelastic Conditions Using Elastic Finite Element Stress Analysis," *Proceedings*, ASME PVP-Vol. 136, Pittsburgh, Pa., 1988.

14 Seshadri, R., and Fernando, C. P. D., "Limit Loads of Mechanical Components and Structures Using the GLOSS R-Node Method," ASME PVP-Vol. 210-2, San Diego, Calif., 1991, pp. 125–134.

15 Boyle, J. T., and Spence, J., *Stress Analysis for Creep*, Butterworths, 1983.

16 Calladine, C. R., *Plasticity for Engineers*, Ellis Horwood Ltd., Chichester, 1985.

17 DeSalvo, G. J., and Gorman, R. W., *ANSYS User's Manual*, Swanson Analysis Systems Inc., USA.

18 Robinson, M., and Gill, S. S., "Limit Analysis of Flush Radial and Oblique Cylindrical Nozzles in Spherical Pressure Vessels. Part I: A Parametric Survey of Results," *International Journal of Pressure Vessel and Piping*, Vol. 1, No. 3, July 1973, pp. 199–231.

19 Palusamy, S., "Limit Pressure of Spherical Shells Subjected to External Axial Force," *Nuclear Engineering Design*, Vol. 16, 1971, pp. 13–23.

20 Mackenzie, D., Shi, J., and Boyle, J. T., "Finite Element Modelling for Limit Analysis by the Elastic Compensation Method," *Computers & Structures*, under review.